ADVANCED MATERIALS INTERFACES
www.advmatinterfaces.de

Directional Water Transport Fabrics with Durable Ultra-High One-Way Transport Capacity

Chao Zeng, Hongxia Wang, Hua Zhou, and Tong Lin**

Fabrics with automatic one-way water transport ability are highly desirable for applications in daily life, industry, health, and defense. However, most of the studies on one-way water transport fabrics only report the qualitative water transport results. The lack of quantitative measure makes it hard to assess the directional transport quality. Here, it is proved that a hydrophilic fabric after being electrosprayed with a thin layer of hydrophobic coating on one side shows one-way water transport ability. By using moisture management tester, the water transport property is qualitatively characterized and the effect of hydrophobic fabric layer thickness on one-way water transport feature is examined. The hydrophobic fabric layer thickness is found to play a key role in deciding the one-way transport ability. When a plain woven fabric with an overall thickness of 420 µm and average pore size of 33 µm is used as fabric substrate, a hydrophobic fabric layer thickness between 22 and 62 µm allows the treated fabric to show a one-way droplet transport feature. A one-way transport index as high as 861 can be attained. The one-way water transport is durable enough to withstand repeated washing. This novel fabric may be useful for development of "smart" textiles for various applications.

1. Introduction

Directional water motion (also referred to as "one-way" water motion) guided by structure and/or surface feature has been observed in nature on plants and insects. A good example is *Stenocara* beetle's wings which have an incredible ability to collect tiny water from the air for its survival in Namib Desert.[1,2] Spider silk with alternate variations of hydrophilicity/hydrophobicity and diameter is another example showing water harvesting ability.[3,4] Water on *Cactus*,[5] *Strelitzia reginae* leaf,[6] and rice leaves[7] also shows directional motion, which is driven by the structural feature. Inspired by these natural examples, advanced water harvesting materials[2,4,5,8] and microfluidics[9,10] have been developed.

Recently, fabrics capable of unidirectionally transporting water across the thickness have been reported. Two main strategies have been developed to prepare directional water transport fabrics: (1) creating a hydrophobicity-to-hydrophilicity gradient through fabric thickness, and (2) combining a layer of hydrophobic fibers with a layer of hydrophilic fibers. For example, Wang et al. and Zhou et al. from our group[11–13] and Kong et al.[14] have separately reported the preparation of directional water transport fabrics through a two-step process involving superhydrophobic treatment of fabric followed by one-side photo-degradation to create a hydrophobicity-to-hydrophilicity gradient through fabric thickness. Zhang et al.[15] used a phase separation method to form a hydrophilic-to-hydrophobic gradient membrane showing directional water transport ability. Wu et al.[16] prepared a directional water transport nanofiber membrane by two-step electrospinning of hydrophobic and hydrophilic nanofibers. Wang et al.[17] in our group prepared a directional oil transport nanofibrous membrane using a layer of oleophobic nanofibers and a layer of oleophilic nanofibers for oil–water separation. Tian et al.[18] reported a vapor-phase method to deposit a fluoroalkyl silane on one side of cotton fabric. The fabric after treatment showed directional water gating behavior in air–water system. However, most of the studies only reported the qualitative results of directional water transport. The lack of quantitative measure makes it hard to assess directional water transport quality. In addition, washing durability is an important feature for practical applications of functional textiles, but little is reported on the directional water transport fabrics.

Apart from experiment development, theoretical understanding of directional water transport fabrics has been performed. Directional water transport through fabrics is ascribed to isotropic wettability along the fabric thickness.[3,11,13,14,19] Directional water transport fabrics show difference in water breakthrough pressure on the two fabric sides.[11–13,17] However, the lack of effective technique to precisely control the coating layer thickness has confined the study on the role of hydrophobic fabric layer thickness in forming directional water transport on conventional fabrics.

Electrospraying is a simple technique to prepare functional coating on solid surface. It involves atomization of liquid under a strong electrical field. Liquid drops split into tiny droplets before depositing on the substrate.[20–23] Electrospraying has been used widely in areas such as ink-jet printing,[24,25] fabric functionalization,[23,26–41] making biomimetic materials,[42,43] and fabricating fuel cells.[44] Since the deposition rate can be controlled through adjusting the flow rate of liquid, electrospraying offers opportunities to control the coating depth on fabric, which is useful for making directional water fabrics. Nevertheless, work on using

C. Zeng, Dr. H. Wang, Dr. H. Zhou, Prof. T. Lin
Institute of Frontier Materials
Deakin University
Geelong, VIC 3216, Australia
E-mail: hong.wang@deakin.edu.au;
tong.lin@deakin.edu.au

DOI: 10.1002/admi.201600036

electrospraying to make one-way water transport fabrics has not been reported. In our previous study, we have used SU-8, a commercial photoresist, and its blends with fluoroalkyl silane and silica nanoparticles to prepare superhydrophobicity.[45] By dip coating SU-8 on a fabric substrate and subsequent UV irradiation, the coated fabric showed an isotropic hydrophobicity with a water contact angle (CA) of 131°.

In this study, we for the first time prove that a hydrophilic fabric after being electrosprayed with a thin layer of SU-8 on one fabric side shows a one-way water transport property. By using moisture management tester (MMT), we have conducted a qualitative study on water transport property and examined the effect of SU-8 coating thickness on water transport feature. It was interesting to note that SU-8 coating layer thickness played a critical role in deciding the transport ability. When a plain woven fabric with an overall thickness of 420 µm and average pore size of 33 µm was used as fabric substrate, a hydrophobic fabric layer thickness between 22 and 62 µm allowed the treated fabric to have a one-way droplet transport feature. A one-way transport index as high as 861 can be attained by the SU-8 coating. The directional water transport fabric was durable against repeated washing.

2. Results and Discussion

Figure 1a shows the chemical structure of SU-8 and fabric treatment procedure. Polyester fabric was pre-treated by immersing in an aqueous NaOH to hydrolyze the fiber surface. The NaOH pre-treatment showed little effect on fiber surface morphology (see fiber morphology in Figure S1, Supporting Information). However, the water contact angle of the polyester fabric after NaOH treatment was changed from 118° to 0°.

It is known that alkali treatment leads to hydrolysis of ester links in polyester to form carboxylic and hydroxyl groups. At a suitable condition, the reaction just happens onto polyester fiber surface (see the chemical reaction and illustration of surface treatment in S1, Supporting Information). Because carboxylic and hydroxyl groups are water absorbing, their presence makes the treated fibers have a hydrophilic surface. Using NaOH to improve the water wettability of polyester fabric has been reported by other researchers,[46–48] despite the treatment method is slightly different.

SU-8 solution was then deposited on one side of the NaOH pre-treated fabric using an electrospraying technique. To prove the coating evenness, a red dye was added into the SU-8 solution for spraying treatment. As shown in Figure 1b, after one-side electrospraying, the fabric is uniformly covered with a layer of red substance just on the sprayed surface, whereas the unsprayed side still preserves the original color. SEM imaging indicated that a thin conformal coating was formed only on the electrosprayed fiber surface (Figure 1c,d, also see Fourier transform IR results in Figure S2, Supporting Information).

Figure 1e,f shows dropping water on either side of the SU-8 sprayed fabric (SU-8 loading, 0.6 g m^{-2}). On the SU-8 sprayed side, water drop (volume, 40 µL) moved spontaneously through the fabric and spread into the non-sprayed surface (Figure 1e). The whole droplet transfer took around 2.5 s. When the same

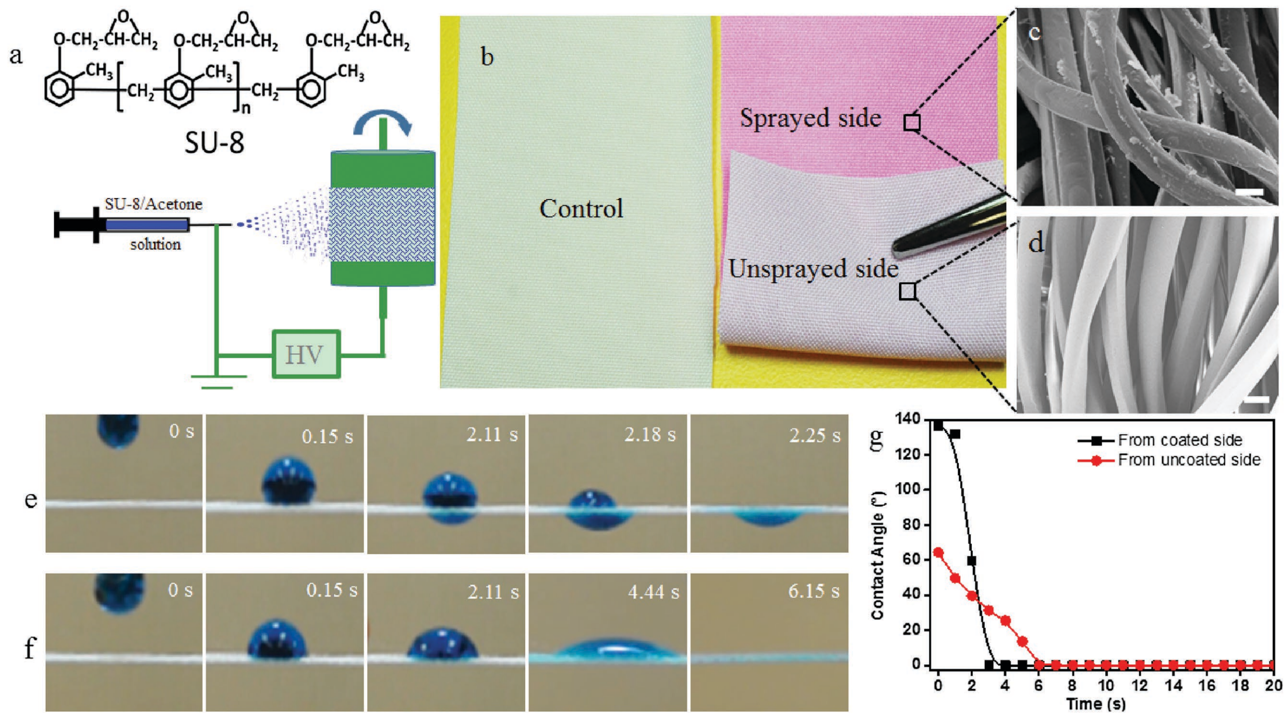

Figure 1. a) Chemical structure of SU-8 and schematic of one-side electrospraying treatment; b) photos of polyester fabric after NaOH-treated (control) and one-side electrospraying treatment with SU-8 (a red dye was added to SU-8 solution to indicate the coating layer); c,d) SEM images of the electrosprayed and un-electrosprayed fabric sides (scale bar, 20 µm); still frames from digital videos to show dropping blue-dyed water on electrosprayed polyester fabric e) on the SU-8 sprayed surface and f) on the unsprayed back surface; and g) water CA change during dropping water on the electrosprayed fabric.

volume of water was dropped on the unsprayed side, however, it just spread on the surface layer without penetrating to the other side. This spreading took around 6 s. Figure 1g shows water CA change during dropping water on the sprayed fabric. On the SU-8 sprayed side, CA changed from 138° to 0° within 3 s, while the CA on the unsprayed surface dropped from 64° to 0° within 6 s. Although CA on both sides showed a reduced trend, they came from different water transport features. On the SU-8 sprayed surface, water penetrated the coating and wicked into the uncoated fabric matrix, whereas water on the un-sprayed side spread directly into the fibrous matrix because of the hydrophilic nature of the pre-treated fabric.

In addition, we also used a dip-coating method to apply SU-8 to the entire polyester fabric (similar to our previous work[45]). The dip-coated fabric showed hydrophobic on both fabric sides (water CA = 131°), but no directional water transport occurred on the fabric (see Figure S3, Supporting Information). A MMT was employed to quantitatively characterize water transport profile on polyester fabrics. **Figure 2**a shows the basic principle of MMT. A fabric sample was placed horizontally between two arrays of moisture sensors. During testing, a small volume (0.15 g) of saline water (0.9% NaCl in deionized (DI) water)[49] was dropped to the top center of the sample. The areas which were wetted with the saline water increased the local conductivity considerably. Through measuring the conductivity change on the two fabric sides, the relative water content (unit %) based on the dry state was obtained, which was reported directly by the MMT (see measurement principle in refs. [50] and [51]).

Figure 2b shows the relative water content on the two sides of the electrosprayed fabric. When water was dropped on the SU-8 sprayed surface, the relative water content on the dropping surface which had SU-8 remained 0 until 56 s. After that the content value increased slowly to 30% at 120 s. However, the relative water content on the lower surface without SU-8 increased rapidly. In 7 s, the water content increased to 500%. After a small decrease at 20 s, it increased slowly to 623% at 120 s. This indicates that water rapidly penetrates through the fabric from the SU-8 coated surface and spread into the uncoated fabric matrix.

Figure 2c shows the relative water content of saline water on the fabric with SU-8 coated side faced down in the MMT. Once water was dropped on the fabric, the water content on the uncoated surface started increasing, and the content reached 1000% in 20 s. When water supply stopped, water content on the uncoated surface decreased rapidly until 60 s, after which the content stabilized at around 500%. In comparison, water content on the SU-8 sprayed surface started increasing at around 7 s, and reached the maximum value (600%) at 30 s. The content then reduced and finally stabilized at 400%. It was expected that the water content measured on the SU-8 sprayed side should be very low because of the high hydrophobicity. This unexpectedly high water content on the SU-8 treated hydrophobic side was attributed to the measurement method. Due to the sensor tips slightly infiltrated into the fabric matrix (depth around 60 µm), the water content measured was actually the bulk content water in the surface layer around 60 µm.

To gain better understanding of the MMT result, we tested the uncoated and NaOH pre-treated polyester fabrics. Both fabrics showed similar water content profile between the two sides, though the water content on the two fabrics changed with time in different trends (Figure S4, Supporting Information). This can be explained by the different wettability of the fabrics. In addition, we tested water content on SU-8 dip-coated fabric, which showed similar water content profile on the two sides as well (Figure S5, Supporting Information).

The MMT also reported wetting time, maximum wet radius, spreading speed, and one-way transport index (also referred to as R value). The R (%) is calculated by the equation

$$R = \frac{1}{T_0}\int [U_b(T) - U_t(T)]\,\mathrm{d}T \tag{1}$$

where U_t and U_b are the relative water content (%) of the fed (i.e., top layer in the MMT tester) and the back layer (i.e., bottom

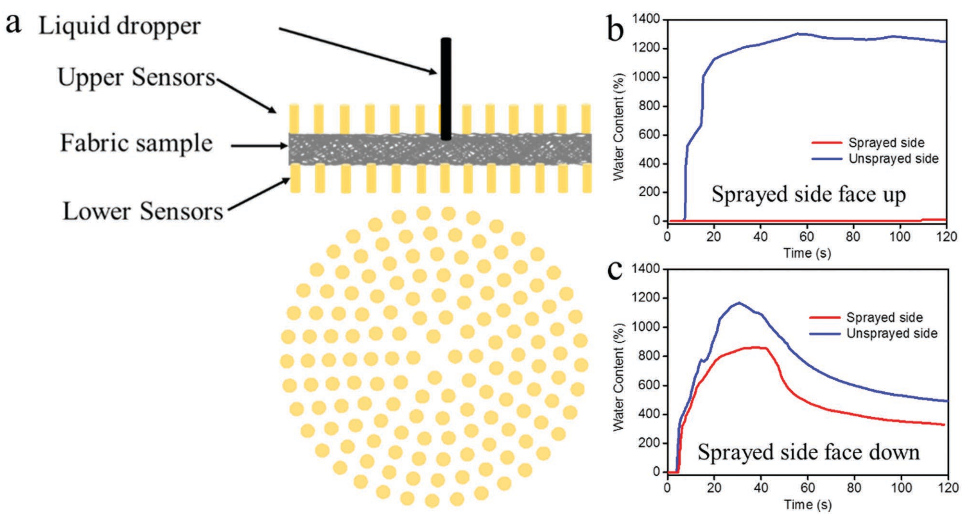

Figure 2. a) Sensor arrays in MMT; the relative water content change with time when the salt water was dropped on b) the SU-8 sprayed side (the SU-sprayed side faced up in the MMT) and c) the un-sprayed side (the SU-sprayed side faced down in the MMT). The blue lines in the chats show the water content change on the unsprayed surface, while the red lines show the water content change on the sprayed surface.

layer and top layer), respectively. T is the total testing time (s). For nominal fabrics which have isotropic wettability, their R values on the two fabric sides are very similar. For the one-side electrosprayed fabric, an R value over 850 on the sprayed side, whereas the R value on the unsprayed side was –157 (Table S1, Supporting Information). Such a large difference in R value between the two fabric surfaces suggests that water will always move toward the un-sprayed fabric matrix no matter on which side the fabric is fed. This also forms an important sign of one-way water transport feature. Since moisture transport is a critical property deciding the thermo-physiological characteristic of garment, one-way water transport allows rapid removal of sweat from skin side to external garment surface. Fabrics with a high R value will improve perspiration when people are excessively sweating such as in tropical climates or during heavy physical work and hence regulating body surface temperature. This could enhance people's endurance against high temperature and nervous perspiration, maintain the wearers in high competitive state, and reduce the chances to get heat stress. We also compared our fabrics with those reported to have a high water transport feature.[46,48–54] Most of the fabrics showed an R value far below 600, and they have no directional water transport either. The high R value enables directional water transport fabrics very useful for making high-performance summer clothing, sportswear, special workwear, and soldier uniform.

To observe the anisotropic wettability, we used micro-computed tomography (μ-CT) technology to characterize the thickness of hydrophobic fabric coating. **Figure 3**a shows a typical μ-CT image of an electrosprayed fabric sample. To increase the image contrast between the hydrophilic and the hydrophobic parts, the fabric was wetted with water. Since the NaOH pre-treated polyester fibers were wettable, the fiber matrix can be fully wetted with water, whereas the SU-8 coated area was hydrophobic and non-wettable. Therefore, water just stay in the uncoated matrix. Figure 3b shows a cross-sectional view taken from the 3D image. The wetted area was brighter than the non-wetted part. The thickness of the non-wetting layer, which was coated with SU-8, can be seen in the image. Based on the image, the hydrophobic fabric layer thickness formed by SU-8 coating can be estimated as 60 ± 5 μm.

Apart from μ-CT, laser scanning confocal microscopy (LSCM) imaging was also employed to observe the SU-8 sprayed fabric and verified the SU-8 coated fabric thickness (Figure 3c). To distinguish the SU-8 coating from the uncoated area, a fluorescence indicator (Rhodamine B) was added into SU-8 coating solution for electrospraying. The light blue area clearly indicated that a thin SU-8 coating was formed on one side of the fabric, and the coating thickness was around 64 μm. In addition, optical microscopy was also used to observe the SU-8 coating layer (Figure S6, Supporting Information).

The above presented result was based on the SU-8 electrosprayed fabric with a SU-8 loading of 0.6 g m^{-2}. By adjusting the electrospraying time, the SU-8 loading weight on the fabric varied (see Figure S7, Supporting Information). We noted that the variation of SU-8 loading on one side of the NaOH pre-treated fabric made the fabric have different water transport features. **Table 1** indicates water transport feature of SU-8 coated fabric at different SU-8 loadings. It was interesting to note that one-way water transport happened when the SU-8 loading on one side of the fabric was in the range of 0.4–1.0 g m^{-2}.

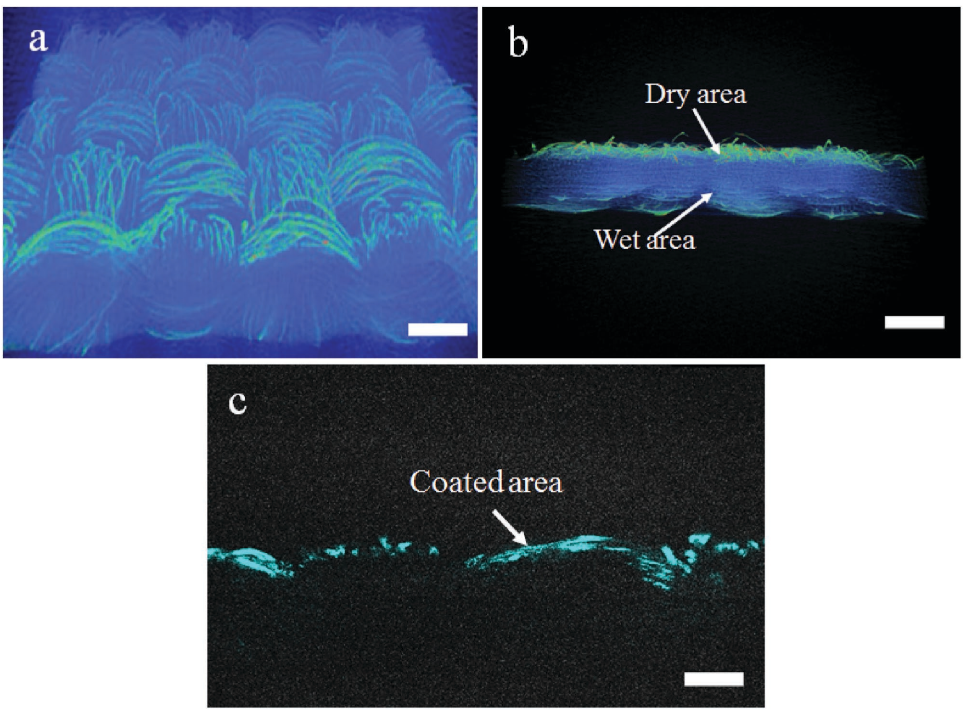

Figure 3. a) Typical μ-CT image obtained from the water-wetted fabric sample (SU-8 electrosprayed); b) 2D cross-sectional images obtained from the μ-CT image; c) confocal microscopy image with Rhodamine B in the SU-8 coating. (Scale bar: 250 μm, the brighter areas in the images a) and b) indicate the non-wetted areas and SU-8 coated area in c).

Table 1. Effect of SU-8 loading weight on water transport feature, coating depth, and *R* value.

SU-8 loading [g m^{-2}]	Water transport ability	VCA [°]		SU-8 coating depth [μm]	R value
		Sprayed side	Unsprayed side		
NaOH treated	Two-way transport	30.7° ± 4.3°	30.6° ± 3.1°	0	78
0.2	Two-way transport	42.0° ± 1.2°	32.0° ± 1.7°	22.4	290
0.6	Directional transport	70.0° ± 2.2°	36.0° ± 1.8°	58.5	861
2.0	None transport	137.0° ± 1.2°	41.0° ± 2.5°	71.6	−1262
SU-8 dip-coated	None transport	132.3° ± 3.1°	131.4° ± 3.2°	410.0	−1240

When the loading was below the lower limit, the fabric still showed two-way water transport feature. However, when the loading was larger than the upper limit, water cannot penetrate through the fabric matrix from both sides. The fabric with a SU-8 loading of 0.6 g m^{-2} showed the best directional water transport effect.

When the SU-8 sprayed fabric samples were vertically dipped in water, they showed different water contact profiles, depending on the loading weight of SU-8. Asymmetric cross-sectional wetting profile results for the SU-coated fabric at a low SU-8 loading weight (0.2 g m^{-2}) are shown in **Figure 4**. On the un-sprayed side, the apparent water–fabric contact (also referred to as "vertical contact angle" (VCA) in this paper) was around 32°, while the SU-8 coated side shows a slightly increased VCA, being around 42°. With increasing SU-8 loading weight to 0.6 and 2.0 g m^{-2}, the VCA on the SU-8 coated side increased to 70° and 137°, respectively. However, the uncoated side still maintained a low VCA value. For comparison, we also tested vertical wetting profile of the control fabric (i.e., NaOH pre-treated polyester) and SU-8 dip-coated fabric. As expected, both fabrics showed almost symmetric VCA, and they had different VCA values, 30° and 131° for the control and the SU-8 dip-coated fabric, respectively.

Using μ-CT, we measured the SU-8 coating depth at different SU-8 loading weights. As listed in Table 1, the coating depth increased with increasing SU-8 loading. Directional water transport took place when the coating depth was 58.5 ± 2.5 μm. When SU-8 coating depth was below 22.4 μm, water could transfer through the fabric from both sides (i.e., bidirectional water transport), whereas the fabric became impermeable to liquid water from either side (i.e., non-transport) when the coating was deeper than 71.6 μm. In addition, the *R* value changed with the SU-8 coating depth. The variation of coating depth between 22.4 and 71.6 μm led to a change of the *R* value in the range of 290–860. Therefore, the moisture transport feature of single-side electrosprayed fabric can be adjusted by changing the SU-8 coating depth.

To further understand the effect of SU-8 coating depth on the fabrics, we measured the initial pressure needed for liquid water to break through the fabric. For the fabric with a one-way water transport ability, the breakthrough pressure on the hydrophobic side was often lower than that on the hydrophilic side.[11,16] For the fabric with SU-8 coating depth around 58 μm, the breakthrough pressure on the SU-8 coated and uncoated sides was 3.17 ± 0.29 and 13.67 ± 1.61 cmH_2O, respectively. This result is in good accordance with our previous reports.[13] When the loading was higher than 1.0 g m^{-2} (i.e., coating depth 62 μm), the breakthrough pressure on the uncoated side was larger than that on the SU-8 coated side (Figure S9, Supporting Information). We also calculated the breakthrough pressure difference ($\Delta P_{uncoated\text{-}coated}$) between the uncoated and the SU-8 coated sides (Figure S10, Supporting Information). When the loading was in the range of 0.4–0.8 g m^{-2}, a large positive ΔP is obtained. However, once the loading was higher than 1.0 g m^{-2}, $\Delta P_{uncoated\text{-}coated}$ became negative, suggesting the disappearance of the directional water transport effect. Therefore, directional water transport could take place only when the SU-8 coating depth is lower than 62 μm.

When water is dropped on fabric, it will either spread into fabric matrix or suspend on surface layer depending on the

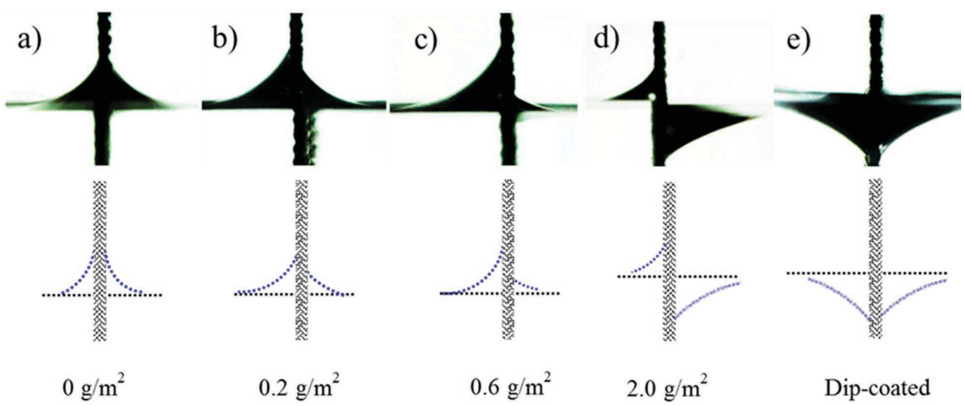

Figure 4. Cross-sectional view (first line) and corresponding cross-sectional wetting profile (second line) of vertically laid fabrics in water, the fabric samples were one-side electrosprayed with SU-8 of loading, a) 0, b) 0.2, c) 0.6, and d) 2.0 g m^{-2}; e) the result on the fabric dip-coated with SU-8.

wettability of the fabric. A gas-solid-liquid three phase equilibrium reaches eventually. It is easily understood that water just spreads on the un-sprayed surface layer because of the hydrophilic nature. In general, water does not spread on hydrophobic surface. However, when water was dropped on the SU-8 coated side, which has a hydrophilic surface, it penetrated through the fabric and spread in the un-spread hydrophilic fabric layer. This can be explained by the stronger surface energy of hydrophilic matrix, allowing water to move across the hydrophilic barrier. In our previous paper, we have pointed out that this directional water transport feature originates from asymmetric wettability across the thickness.[11–13]

In the previous studies, we have proposed the mechanism of directional fluid transport.[11,13] Water transport through the SU-8 sprayed fabric is illustrated in **Figure 5**. It is easy to understand that water can easily spread into the hydrophilic matrix when it is dropped on the un-sprayed side. However, water can only penetrate the un-treated matrix, and its penetration is blocked once it meets the SU-8 treated fibers because the hydrophobic fibers generate a reverse capillary force. When water is dropped on the SU-8 sprayed surface, which is hydrophobic, it receives a remote capillary force from the hydrophilic matrix behind, which draws the liquid to overcome the hydrophilic barrier layer and spread into the hydrophilic layer.

In addition, we tested the washing durability of the directional water transport fabric. After 50 cycles of repeated washing, the coating was still on one side of the fabric surface (Figure S11, Supporting Information) and the fabric still showed a directional water transport feature similar to the unwashed fabric (Table S1, Supporting Information). This indicates that directional water transport fabric prepared by one-side electrospraying of SU-8 has reasonable durability against washing. This good durability should come from the excellent durability of SU-8 coating on fabrics.[45]

Such a fabric will be very useful for making sportswear, summer clothing, and workwear. Sweating during heavy physical work or exercise, especially in a hot or humid environment, is often uncomfortable, especially when the fabric clings to the skin. Our directional water transport fabrics will be an effective solution to this problem. The fabric functions as a second skin to proactively move sweat from the skin to outer fabric surface because of the directional transport feature. This accelerates moisture evaporation, and creates a dry, comfortable microenvironment to the wearer.

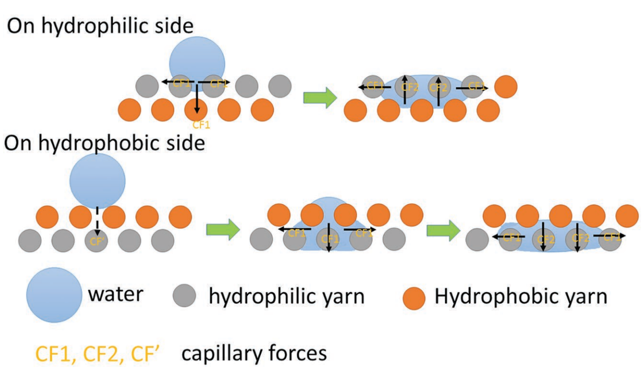

Figure 5. Schematic illustration of the directional water transport mechanism.

3. Conclusion

We have proven that a hydrophilic fabric after being one-side electrosprayed with a hydrophobic resin can have a directional water transport ability. The hydrophobic fabric layer thickness plays a critical role in deciding the directional water transport ability. For SU-8 on hydrophilic fabric, the fabric shows directional water transport property only when the SU-8 coating is in the specific range of thickness. For a plain woven fabric with an overall thickness of 420 µm and average pore size of 33 µm used as fabric substrate, a hydrophobic fabric layer thickness between 22 and 62 µm allowed the treated fabric to show a one-way droplet transport feature. Such a one-side SU-8 coating allows the treated fabric to have a one-side transport index as high as 860 on the coated side and nearly 1000 of *R* value difference between the two surfaces of the fabric. Fabrics with directional water transport property have an asymmetric wetting profile on the two sides. These new understandings may be useful for designing and developing novel "smart" textiles for various applications.

4. Experimental Section

Materials: NaOH and Rhodamine B were purchased from Aldrich. SU-8 2075 was provided by Microchem Corporation. Commercial polyester fabric (plain weave, 168 g m^{-2}, thickness = 420 µm) was used as substrate. The polyester fabric was pre-treated with 10% aqueous NaOH at 60 °C for 25 min to hydrolyze the surface layer. After pretreatment, the fabric was rinsed with water, 3% acetic acid solution, and water again, and finally dried at room temperature in air for 24 h.

Coating Treatment: The pretreated fabric was coated with SU-8 on one side using a purpose-built electrospraying device. To prepare fluorescent-labeled samples for confocal microscopy measurement, Rhodamine B (4 wt%) was added to SU-8 coating solution. The coated fabric was irradiated by UV light (80 mW cm^{-2}) for 10 min, then heated at 120 °C for 10 min and finally 95 °C for 1 min.

Characterizations: Water contact angles were measured on a contact angle goniometer (KSV CAM 101). Water drop for the measurement was 5 µL in volume. SEM imaging was performed on Supra 55VP operated under 10 kV acceleration voltages. Confocal microscope images were obtained on LSCM (Leica TCS SP5, Germany). Laser at a wavelength of 543 nm was used to excite the Rhodamine B-labeled coating. The 3D structure of the fabric samples was obtained on an X-ray µ-CT (XRadia, USA). The samples were scanned at a rotation stage from 0.25° to 180°. Finally, 512 projections with a spatial resolution of 1.155 µm were obtained under 30 s projections of exposure time. Breakthrough pressure was measured by a purpose-built device comprising a fluid-feeding system, a pressure gauge, and a fabric holder. During measurement, deionized water was loaded at a flow rate of 25 mL min^{-1} and the minimum pressure under which the fluid started passing through the fabric was recorded as the breakthrough pressure. Moisture transfer property was measured using a MMT. The specimen was cut into round size of 90 mm^2 and held with sample stages. Saline water (16.6 g, containing 0.9% NaCl, as required by AATCC-15 for MMT testing) was dropped in 20 s onto the upper surface of the fabric sample. The spreading profile (in the first 120 s since starting dropping the saline water) of the saline water on the two sides of the fabric sample was measured by sensor arrays located on the upper and the lower surfaces of the fabric. All samples were put into the conditioned room (21 ± 1 °C, relative humidity 65 ± 2%, refer to ASTM D1776) for at least 24 h prior to testing.

Supporting Information

Supporting Information is available from the Wiley Online Library or from the author.

Acknowledgements

Funding support from Australian Research Council through a discovery project (DP150100406) is acknowledged.

Received: January 15, 2016
Revised: March 29, 2016
Published online:

[1] A. R. Parker, C. R. Lawrence, *Nature* **2001**, *414*, 33.
[2] L. Zhai, M. C. Berg, F. C. Cebeci, Y. Kim, J. M. Milwid, M. F. Rubner, R. E. Cohen, *Nano Lett.* **2006**, *6*, 1213.
[3] Y. Zheng, H. Bai, Z. Huang, X. Tian, F.-Q. Nie, Y. Zhao, J. Zhai, L. Jiang, *Nature* **2010**, *463*, 640.
[4] Z. Huang, Y. Chen, Y. Zheng, L. Jiang, *Soft Matter* **2011**, *7*, 9468.
[5] J. Ju, H. Bai, Y. Zheng, T. Zhao, R. Fang, L. Jiang, *Nat. Commun.* **2012**, *3*, 1247.
[6] E. Mele, S. Girardo, D. Pisignano, *Langmuir* **2012**, *28*, 5312.
[7] L. Feng, S. Li, Y. Li, H. Li, L. Zhang, J. Zhai, Y. Song, B. Liu, L. Jiang, D. Zhu, *Adv. Mater.* **2002**, *14*, 1857.
[8] H. Bai, X. Tian, Y. Zheng, J. Ju, Y. Zhao, L. Jiang, *Adv. Mater.* **2010**, *22*, 5521.
[9] M. Grunze, *Science* **1999**, *283*, 41.
[10] Y. H. Lai, J. T. Yang, D.-B. Shieh, *Lab Chip* **2010**, *10*, 499.
[11] H. Wang, J. Ding, L. Dai, X. Wang, T. Lin, *J. Mater. Chem.* **2010**, *20*, 7938.
[12] H. Wang, X. Wang, T. Lin, *J. Nanosci. Nanotechnol.* **2013**, *13*, 839.
[13] H. Zhou, H. Wang, H. Niu, T. Lin, *Sci. Rep.* **2013**, *3*, 2964.
[14] Y. Kong, Y. Liu, J. H. Xin, *J. Mater. Chem.* **2011**, *21*, 17978.
[15] Y. Zhang, M. Barboiu, *Chem. Commun.* **2015**, *51*, 15925.
[16] J. Wu, N. Wang, L. Wang, H. Dong, Y. Zhao, L. Jiang, *Soft Matter* **2012**, *8*, 5996.
[17] H. Wang, H. Zhou, H. Niu, J. Zhang, Y. Du, T. Lin, *Adv. Mater. Interfaces* **2015**, *2*, 1400506.
[18] X. Tian, H. Jin, J. Sainio, R. H. Ras, O. Ikkala, *Adv. Funct. Mater.* **2014**, *24*, 6023.
[19] X. Tian, J. Li, X. Wang, *Soft Matter* **2012**, *8*, 2637.
[20] J. Carstoiu, *Proc. Natl. Acad. Sci. USA* **1968**, *59*, 326.
[21] M. Cloupeau, B. Prunet-Foch, *J. Electrost.* **1989**, *22*, 135.
[22] M. Cloupeau, B. Prunet-Foch, *J. Electrost.* **1990**, *25*, 165.
[23] S. Islam, A. Jadhav, J. Fang, L. Arnold, L. J. Wang, R. J. Padhye, X. G. Wang, T. Lin, *Adv. Mater. Res.* **2011**, *331*, 165.
[24] J. H. Kim, S. J. Sung, D. K. Hwang, *Appl. Mech. Mater.* **2015**, *705*, 51.
[25] Y. Xu, Y. Zhu, F. Han, C. Luo, C. Wang, *Adv. Energy Mater.* **2015**, *5*, 1400753.
[26] C. Güneşoglu, D. Kut, M. Orhan, *Text. Res. J.* **2010**, *80*, 106.
[27] A. Jadhav, L. J. Wang, C. Lawrence, R. Padhye, *Adv. Mater. Res.* **2011**, *332*, 710.
[28] C. Güneşoglu, S. Güneşoglu, S. Wei, Z. Guo, *J. Text. Inst.* **2011**, *102*, 434.
[29] A. Jadhav, L. J. Wang, C. Lawrence, R. Padhye, *Adv. Mater. Res.* **2012**, *535*, 1146.
[30] A. Jadhav, L. Wang, R. Padhye, *Int. J. Appl. Mech. Mater.* **2013**, *2*, 64.
[31] J. Cuevas, B. Gonzalo, C. Rodríguez, A. Domínguez, D. Galán, I. Loscertales, *J. Exp. Nanosci.* **2014**, *1*.
[32] P. Gibson, H. Schreuder-Gibson, *Am. Soc. Mech. Eng., Mater. Div. [Publ.] MD* **2000**, *91*, 45.
[33] A. Jaworek, A. Krupa, A. Sobczyk, M. Lackowski, T. Czech, S. Ramakrishna, S. Sundarrajan, D. Pliszka, *Solid State Phenom.* **2008**, *140*, 127.
[34] A. Jaworek, A. Krupa, M. Lackowski, A. Sobczyk, T. Czech, S. Ramakrishna, S. Sundarrajan, D. Pliszka, *J. Electrost.* **2009**, *67*, 435.
[35] A. Jaworek, A. Krupa, M. Lackowski, A. Sobczyk, T. Czech, S. Ramakrishna, S. Sundarrajan, D. Pliszka, *Fibres and Textiles in Eastern Europe*, **2009**, *75*, 77.
[36] B. Y. Lee, K. Behler, M. E. Kurtoglu, M. A. Wynosky-Dolfi, R. F. Rest, Y. Gogotsi, *J. Nanopart. Res.* **2010**, *12*, 2511.
[37] N. Vitchuli, Q. Shi, J. Nowak, K. Kay, J. M. Caldwell, F. Breidt, M. Bourham, M. McCord, X. Zhang, *Sci. Technol. Adv. Mater.* **2011**, *12*, 055004.
[38] F. Lijo, E. Marsano, C. Vijila, R. Barhate, V. Vijay, S. Ramakrishna, V. Thavasi, *J. Nanosci. Nanotechnol.* **2011**, *11*, 1154.
[39] M. W. Lee, S. An, B. Joshi, S. S. Latthe, S. S. Yoon, *ACS Appl. Mater. Interfaces* **2013**, *5*, 1232.
[40] E. Korina, O. Stoilova, N. Manolova, I. Rashkov, *Macromol. Biosci.* **2013**, *13*, 707.
[41] D. Virovska, D. Paneva, N. Manolova, I. Rashkov, D. Karashanova, *Appl. Surf. Sci.* **2014**, *311*, 842.
[42] A. Taniokia, H. Matsumoto, I. Uematsu, K. Morota, M. Minagawa, Y. Yamagata, K. Inoue, *ACS Symposium Series*, Oxford University Press, **2006**, pp. 343–352.
[43] H. Liu, J. Zhou, D. Zuo, X. Liu, S. Gu, W. Xu, *J. Appl. Polym. Sci.* **2014**, *131*, 40245.
[44] A. Chaparro, P. Ferreira-Aparicio, M. Folgado, A. Martín, L. Daza, *J. Power Sources* **2011**, *196*, 4200.
[45] C. Zeng, H. Wang, H. Zhou, T. Lin, *RSC Adv.* **2015**, *5*, 61044.
[46] Z. Wang, C. W. Macosko, F. S. Bates, *ACS Appl. Mater. Interfaces* **2014**, *6*, 11640.
[47] C. H. Xue, P. Zhang, J. Z. Ma, P. T. Ji, Y. R. Li, S. T. Jia, *Chem. Commun.* **2013**, *49*, 3588.
[48] M. Montazer, A. Sadighi, *J. Appl. Polym. Sci.* **2006**, *100*, 5049.
[49] J. Hu, Y. Li, K. W. Yeung, A. S. Wong, W. Xu, *Text. Res. J.* **2005**, *75*, 57.
[50] Y. Li, W. Xu, P. K. Yeung, Y. L. Kwok, *Moisture Management of Textiles* **2002**, US Patent 6499338B2.
[51] L. Zhou, X. Feng, Y. Du, Y. Li, *Text. Res. J.* **2007**, *77*, 951.